Inherent and Dynamic B_0 Mapping and Deblurring in SENSE Spiral Imaging and Application to Resting-State fMRI

Trong-Kha Truong[1], and Nan-kuei Chen[1]
[1]*Brain Imaging and Analysis Center, Duke University, Durham, NC, United States*

Introduction

Spiral imaging is a fast MRI technique used in applications such as functional MRI (fMRI), including task fMRI and resting-state fMRI, as it benefits from an efficient k-space coverage and a low sensitivity to flow artifacts. It is, however, vulnerable to spatial and temporal variations of the static magnetic field (B_0) caused by susceptibility effects, subject motion, physiological noise, and/or system instabilities, resulting in image blurring. Previously proposed deblurring methods rely on B_0 maps that are either separately acquired (1–5), which increases the scan time and precludes the correction of temporal B_0 variations; estimated from the data (6–8), which is less robust; or derived from modified pulse sequences (9,10), which is limited by a low spatial resolution or reduced throughput. In contrast, a k-space energy spectrum analysis (KESA) method was recently proposed to inherently and dynamically generate a B_0 map from the spiral k-space data at each time point, without requiring any additional data acquisition or pulse sequence modification (11). Here, we further extend this novel method to SENSE spiral imaging and demonstrate its effectiveness in resting-state fMRI experiments.

Methods

In gradient-echo spiral imaging, B_0 inhomogeneities cause distortions of the k-space trajectory, resulting in a shift of the echo peak from the center of k-space and blurring in the reconstructed image. If these B_0 inhomogeneities are spatially nonlinear, the echo shift varies with pixel location and is equal to:

$$\Delta k_x(x, y) = \gamma G_x(x, y)\,\mathrm{TE} \qquad [1]$$

$$\Delta k_y(x, y) = \gamma G_y(x, y)\,\mathrm{TE} \qquad [2]$$

where γ is the gyromagnetic ratio, $G_x = \partial B_0/\partial x$, $G_y = \partial B_0/\partial y$, and TE is the echo time.

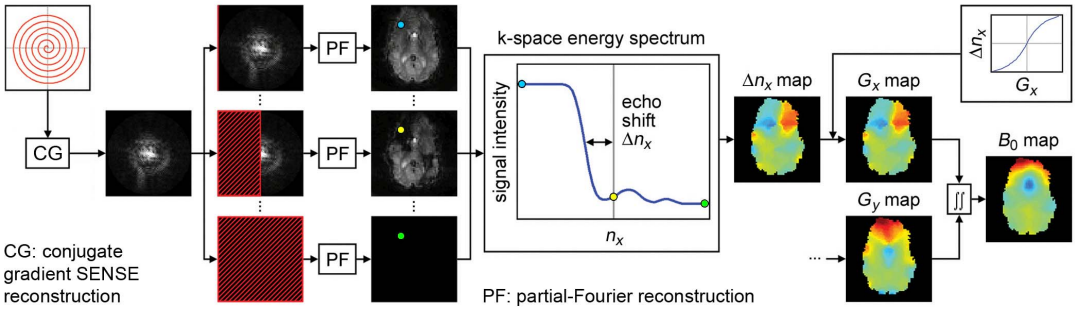

Fig. 1: Schematic diagram of the KESA method for inherent and dynamic B_0 mapping in SENSE spiral imaging.

The proposed KESA method can inherently measure this spatially dependent echo shift from SENSE spiral k-space data to generate a B_0 map. Specifically, the undersampled spiral k-space data are first reconstructed with a conjugate gradient algorithm (12) and Fourier transformed to a fully sampled $N_x \times N_y$ Cartesian k-space (Fig. 1). A number n_x = 1, ..., N_x of k_x lines are then truncated from this k-space data to reconstruct N_x partial-Fourier images. The signal intensity of each pixel is extracted from these images and plotted as a function of n_x to form a "k-space energy spectrum." A sudden drop of signal intensity occurs when the echo peak is truncated and the echo shift is quantified as the number Δn_x of k_x lines between this transition point and the center of k-space. The resulting Δn_x map is converted to a G_x map by using a G_x vs. Δn_x curve derived from Eq. [1]. This procedure is repeated along k_y to generate a G_y map. Finally, the G_x and G_y maps are integrated to obtain a B_0 map, which is used to correct for the blurring in the spiral image. For dynamic applications such as fMRI, this method can generate a B_0 map for each time point to correct for both spatial and temporal B_0 variations.

We studied healthy volunteers on a 3T GE scanner equipped with an 8-channel head coil. High-order shimming was applied to minimize the global B_0 inhomogeneity. Axial images of the whole brain were acquired with a single-shot spiral-in gradient-echo sequence, TR = 2 s, TE = 28 ms, flip angle = 60°, FOV = 24 cm, matrix size = 64×64, slice thickness = 3.8 mm, and SENSE acceleration factor = 2. Five-minute runs were acquired while the subjects were resting with their eyes open. High-resolution T_1-weighted images were also acquired for anatomical reference. Standard resting-state fMRI analysis was used to process the acquired data. The images were first aligned, detrended, low-pass filtered (< 0.08 Hz), and spatially smoothed with a 7 mm Gaussian kernel. Independent component analysis (ICA) was then performed with the FSL MELODIC toolbox to identify various resting-state networks, including the default mode network (specifically the posterior cingulate cortex and the medial prefrontal cortex) as well as the sensorimotor network.

Results and Discussion

Representative results are shown in Figs. 2–3. Even with parallel imaging, the spiral images are still affected by blurring artifacts (Fig. 2a,c). Although such artifacts are most prominent at the anterior and posterior edges of the brain, they also affect other regions inside the brain. The proposed method can effectively correct for the blurring and improve the image quality (Fig. 2b,d). The default mode network derived from the uncorrected data is abnormally asymmetrical in the medial prefrontal cortex (Fig. 3a), whereas the one derived from the corrected data is symmetrical, as expected (Fig. 3b). Similarly, the sensorimotor network also becomes more symmetrical after deblurring (Fig. 3d).

These preliminary results demonstrate that the proposed KESA method can inherently and dynamically correct for the blurring artifacts caused by spatial and temporal B_0 variations in SENSE spiral images and hence improve the spatial fidelity of the resting-state networks derived from these data, without requiring any additional data acquisition or pulse sequence modification. Further work is currently underway to more systematically validate this method in a larger number of subjects.

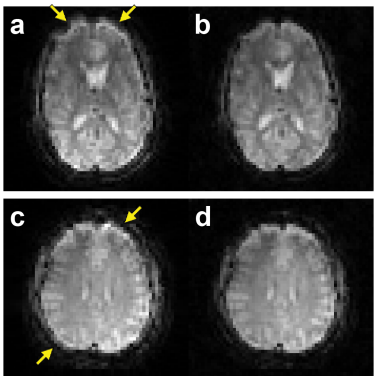

Fig. 2: Uncorrected (left) and corrected (right) SENSE spiral images for two representative subjects.

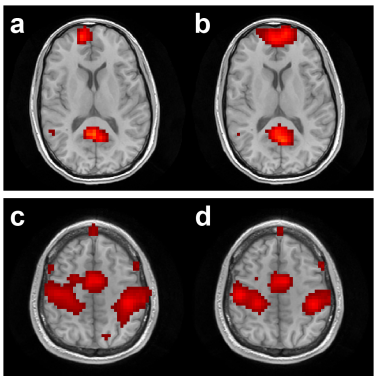

Fig. 3: Uncorrected (left) and corrected (right) default mode network (top) and sensorimotor network (bottom).

References: 1. Noll IEEE TMI 1991;10:629, 2. Irarrazabal MRM 1996;35:278, 3. Man MRM 1997;37:785, 4. Ahunbay MRM 2000;44:491, 5. Sutton IEEE TMI 2003;22:178, 6. Noll MRM 1992;25:319, 7. Man MRM 1997;37:906, 8. Chen MRM 2006;56:457, 9. Nayak MRM 2001;45:521, 10. Sutton MRM 2004;51:1194, 11. Truong MRM 2010;64:1121, 12. Pruessmann MRM 2001;46:638. This work was in part supported by NIH grant EB12586.